IAC-21, C3, 4, 7, x64087

Pyrite as prospective monograin layer solar cell absorber material for *in-situ* solar cell fabrication on the Moon

Taavi Raadik[a*] Katriin Kristmann[a], Mare Altosaar[a], Maarja Grossberg[a], Jüri Krustok[a,b], Maris Pilvet[a], Valdek Mikli[a], Marit Kauk-Kuusik[a]

[a] *Department of Materials and Environmental Technology, Tallinn University of Technology, Ehitajate Tee 5, 19086, Tallinn, Estonia*
[b]*Division of Physics, Tallinn University of Technology, Ehitajate tee 5, 19086 Tallinn, Estonia*
taavi.raadik@taltech.ee
* Corresponding Author

Abstract

Energy is needed in order to keep a Lunar Base on the run and solar energy is one of the most attractive options. There are two ways to achieve it – to bring necessary solar panels from Earth or find the way to produce them *in-situ* on the Moon, from local resources. We propose monograin layer (MGL) solar cell technology, that could be used for the *in-situ* production of solar panels on the Moon. One of the most promising compounds, that can be used as an absorber material in monograin layer solar cell is pyrite FeS_2. There are vast amounts of iron and sulphur in the lunar regolith. Conditions for the synthesis-growth of FeS_2 monograin powders were found and are presented in this study. The recrystallization of FeS_2 powder at 740 °C in KI for a week followed by slow cooling to 575 ºC and rapid cooling to the room temperature, resulted in single phase pyrite monograin powder. Powder crystals had round shape and the median size of about 50 micrometres was appropriate for making monograin layers (MGLs). The produced FeS_2 MGLs were used as absorber layers in MGL solar cells with structure as graphite/FeS_2/NiO/TCO and in FeS_2/Pt Schottky diodes. Charge carrier concentration of 6.2×10^{16} cm^{-3} was determined from *C-V* measurements of FeS_2/NiO heterostructure and $2.5 \times 10^{17} cm^{-3}$ from FeS_2/Pt Schottky diode.

Keywords: monograin layer solar cell, molten salt synthesis, FeS_2, in-situ resource utilization, lunar base

Acronyms/Abbreviations

EDX	Energy-dispersive X-ray spectroscopy
HR-SEM	High resolution scanning electron microscope
ISRU	In-Situ Resources Utilization
MGL	monograin layer
TCO	transparent conductive oxide
KI	potassium iodide
KCN	potassium cyanide
XRD	X-ray diffraction
NiO	nickel oxide

1. Introduction

Securing a permanent lunar outpost is among the goals of future interplanetary space flights and the exploration of Mars and further celestial objects [1], [2]. Therein, establishing reliable energy supply on the Moon will define the feasibility of the mission. It is extremely practical to manage with resources that are available in the lunar soil (or regolith) to lower the price of the lunar village mission.

It is especially important to establish reliable energy supply. Continuous photovoltaic solar energy production is possible on the Moon because some areas around the lunar south pole are constantly illuminated by the Sun [3]. Producing solar cell materials and panels *in situ* from elements of lunar regolith would be the best way to use the available resources, as the cost of sending them from Earth is extremely high [4]. This study was aimed to the *in-situ* resource utilization (ISRU) approach to produce solar energy on the Moon. One promising possibility is to use the monograin layer (MGL) solar cell technology [5]–[7]. The MGL solar cell concept for semiconductor compounds was proposed more than 50 years ago [8]. MGL solar cell has a superstrate solar cell structure: *back contact / absorber / buffer / transparent conductive oxide*. The structure is glued on a supportive substrate (glass or polymer film). The MGL solar cell absorber is a monolayer of nearly unisize semiconductor powder crystals fixed with a thinner than crystal size layer of epoxy (or some other polymer) (Figure 1.) [8]. The MGL

solar cell structure enables to manufacture flexible, lightweight, and cost-efficient solar panels. The technology combines the advantages of high-efficient single-crystalline material and of low-cost roll-to-roll panel production. MGL technology allows to cover vast areas with minimum cost [8]. Before MGL preparation the powder crystals' surfaces are coated with thin layer of a buffer material (ordinarily via solution deposition under continuous stirring) for creating *p/n junction*. After buffer layer deposition (followed by soft heat-treatment) each covered crystal is a tiny photovoltaic cell, ready to be bound into monograin membranes. Therefore, the MGL technology has an advantage compared to all other thin film technologies - it allows to separate (geographically) processes of absorber (powder) production from solar cell module formation. The suitability of MGL solar cells for space applications was evaluated by T. Raadik *et al.* [9], where the tests were made in the conditions simulating lunar environment. Based on the results of work [9] the European Space Agency showed remarkable interest in the monograin solar cell technology due to its advantages.

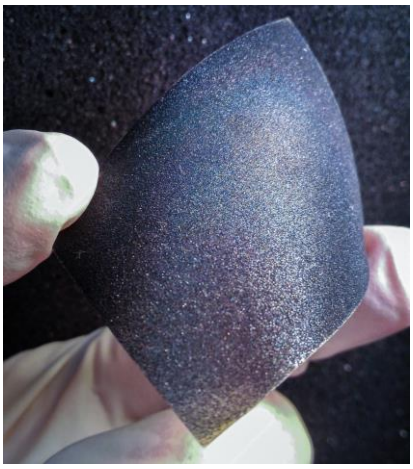

Fig. 1. Semi-finished MGL solar cell without encapsulant

One promising candidate for MGL solar cell absorber material is pyrite (FeS_2). Lunar soil has a high content of iron (Fe) at the lunar mare and sulphur (S) at highland areas [10]. Furthermore, most of the elements that are present on Earth can also be found from the Moon's soil [11], [12]. Therefore, it is possible to harvest most of the necessary elements for solar cell production *in situ* from the lunar soil, starting from absorber material and ending with an antireflective surface coating.

Pyrite is a semiconductor material that has all necessary parameters to be used in an efficient solar cell device. It has a suitable bandgap of 0.85-0.95 eV, high absorption coefficient, high minority carrier diffusion length and an electron mobility up to 360 $cm^2V^{-1}s^{-1}$ at room temperature – all making pyrite attractive as an absorber material to achieve potentially up to 25% energy conversion efficiency [13]–[16]. For FeS_2 synthesis it is necessary to extract iron and sulphur from regolith. According to literature, iron exists in lunar soil in large quantities in the form of silicate and oxide phases. Troilite (FeS) can also be found. So, it is required to add sulphur to FeS to form pyrite (FeS_2). It has been reported that sulphur can be extracted from regolith by heating it at 750-1100ºC [17], [18].

2. Materials and methods

2.1 Synthesis of FeS_2 microcrystals

In this study FeS_2 monograin powders were synthesized from high-purity (5N) FeS and S acquired from Alpha Aesar. The synthesis-growth process was performed in potassium iodide (KI) flux. The amounts of KI and the precursors for FeS_2 formation were weighted considering that the volume of liquid phase V_{liquid} at the process temperature would be at least 0.6 of the volume of solid phase $V_{solid.}$ This volume ratio of liquid and solid phases provides the condition where repelling forces rise and exceed the capillary contracting forces between solid particles. In this case the formation and growth of individual separate crystals is possible [19]. Precursors FeS and S were weighted considering the formation of stoichiometric FeS_2, mixed with KI by grinding in a mortar and loaded into a quartz ampoule. After degassing and heating up to approximately 80 ºC the ampoule was sealed and heated in a furnace at 600 ºC for 48 hours. After that, the furnace temperature was increased to 740 ºC and kept at this temperature for one week. Then the furnace with ampoule was slowly cooled to 575 °C to ensure the pure FeS_2 pyrite phase in accordance with the published iron-sulphur phase diagrams [20], [21]. The furnace was kept at 575°C for 24 hours. After that the ampoules were rapidly cooled by quenching in water. As KI is water-soluble, leaching with DI water under ultrasonic agitation was used to release FeS_2 crystals from solid KI flux. Powders were rinsed multiple times until washing water remained clear and transparent. Reliability of the synthesis-growth process was confirmed by repeating it several times. The produced FeS_2 powder samples were very similar to each other and had a uniformly high quality.

2.1 Deposition and properties of NiO buffer layer

As synthesized pyrite FeS_2 microcrystals exhibited *n*-type conductivity by detecting with the hot probe method, a *p*-type partner was needed for *p/n* junction. NiO was chosen as an option for the buffer layer, as it is a common *p*-type semiconductor material, has a wide bandgap in the range of 3.6–4.0 eV [22] and utilizes abundant nontoxic elements that are readily available in

the lunar soil [10]. NiO buffer layer was deposited by the successive ionic layer adsorption and reaction (SILAR) method from RT $NiSO_4$ solution. NiO deposition based on the recipe proposed by Akaltun et al. [22] that utilized a 0.1 M Ni^{2+} solution and hot water (85°C) for NiO formation. Ni^{2+} ions in this solution were in complex with NH^{4+} ions, while the ratio of [Ni^{2+}] to [NH_4^+] was equal to 1:10. The NiO deposition from 0.1 M Ni^{2+} solution was quick and the deposited layers had cracks. Therefore, the $NiSO_4$ solution was diluted to 0.02 M to achieve thinner films with better coherence. [Ni^{2+}] : [NH_4^+] equal to 1:10 was kept constant and different deposition cycles of SILAR (20, 40 and 60 cycles) were applied for depositing films of different thickness, having continuous coverage and high transmittance.

2.2 Production of FeS_2 Schottky diodes and solar cells

Schottky diodes were prepared to measure their current-voltage characteristics and determine pyrite crystals' work function and Fermi level. As FeS_2 has work function of 3.9 eV [23] then Pt with work function of 6.1 eV [24] was considered as a suitable metal junction partner for pyrite. The FeS_2 monograin membranes for Schottky diodes and FeS_2/NiO hetero-structures were made from sieved FeS_2. The size fraction of 45-56 micrometers was used. Powder crystals were halfway embedded into a thin layer of epoxy leaving upper half of the crystals nondetached with epoxy and then covered with a junction partner material – metal or semiconductor. Pt layer was deposited by sputtering, NiO was deposited by the SILAR method.

2.2 Characterization of FeS_2 microcrystals and NiO films

The phase composition of the synthesized FeS_2 powders was studied by X-ray diffraction (XRD) and by Raman spectroscopy. In Raman studies the Horiba's LabRam HR800 spectrometer equipped with a multichannel CCD detection system in the backscattering configuration was used. 532 nm laser line with spot size of 5 mm was applied for excitation. XRD patterns were recorded on a Rigaku Ultima IV diffractometer with Cu K_α radiation (λ=1.5406 Å). PDXL 2 software was used for the derivation of crystal structure information from the recorded XRD data. The chemical composition of powders was determined by energy dispersive X-ray spectroscopy (EDX) using Bruker Esprit 1.8 system. EDX analyse was performed over the crystals' surface to investigate the elemental distribution and compositional uniformity of different microcrystals. The morphology of crystals was studied with the high-resolution scanning electron microscope (HR-SEM) Zeiss ULTRA 55.

2.3 Characterization of Schottky diodes and solar cells

To evaluate the main electrical characteristics of our devices, current-voltage characteristics were measured in darkness and under illumination. under AM 1.5 G (100 mW/cm^2) using a Newport Class AAA solar simulator system. *I–V* characteristics were recorded by a Keithley 2400 source meter.
Carrier density of pyrite in devices was determined from capacitance-voltage measurements using Wayne Kerr 6500B potentiostat at different frequencies between 0.01 MHz to 10 MHz.

4. Results and Discussion

4.1 Recrystallization of FeS_2 crystals in KI flux

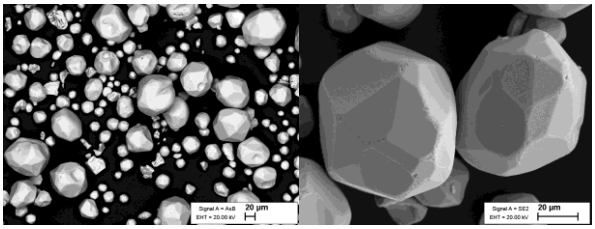

Fig. 2. SEM images of FeS_2 crystals recrystallized in KI flux at 740 °C

The FeS_2 powder synthesized from FeS and S (see the previous chapter) was recrystallized in KI as flux at 740 °C for one week. Formed crystals had a uniform round shape and smooth surfaces (see Fig. 2) – the morphology is suitable for monograin layer production. Roughly half of the gained powder material was in the desired size fraction of around 50 microns.

4.3 Raman, EDX and XRD results

Raman spectra of microcrystals recrystallized in KI at 740 ºC can be seen in Fig. 3. Raman peaks at 343, 379 and a weak peak at 430 cm^{-1} are characteristic to the pyrite phase as reported in the literature [25], [26]. Based on Raman analysis (Fig.3) it can be concluded that the recrystallization of FeS_2 powder at 740 °C in KI followed by slow cooling to 575 ºC resulted in pure FeS_2 pyrite phase. It is possible to avoid the formation of secondary unwanted iron sulphide phases if to proceed at high temperatures, provide the conditions for phase transition, quench the material quickly and use a flux material that can be removed by leaching and rinsing with water [27].

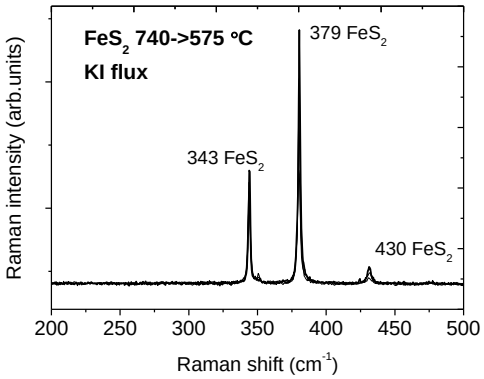

Fig. 3. Raman spectra of FeS_2 crystals recrystallized at 740 °C in KI flux. Flux is removed by dissolution in water.

According to the EDX results crystals recrystallized at 740 °C had average composition of 33.71 at. % iron and 66.29 at. % sulphur. The results were practically same to the crystals surface and bulk composition.
Finally, the microcrystals recrystallized at 740 ºC were analysed by XRD. The XRD pattern is presented in Figure 4. The recorded lattice parameters a = b = c = 5.4154 Å confirm the cubic structure and are in good accordance with values reported in the literature [28]–[30]. Additionally, XRD supports the Raman results that there are no secondary phases in the crystals recrystallized at 740 °C in KI flux.

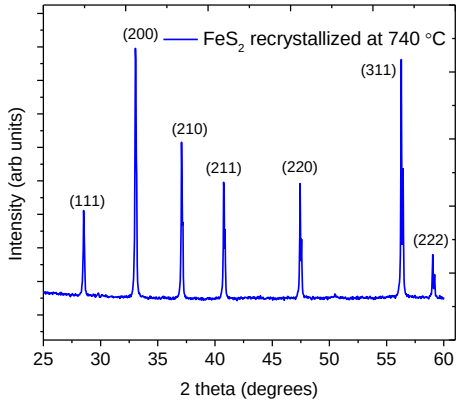

Fig. 4. XRD pattern of FeS_2 powders recrystallized at 740 °C in KI flux.

4.4 Electrical properties of the pyrite devices

Pyrite based Schottky diodes with Pt as junction partner were studied to assess the creation of a rectifying junction.

I -V curve of the structure of FeS_2/Pt is presented in Figure 5 (blue line). It can be seen from the *I-V* curve shape that a small rectifying junction is formed. However, the determination of built-in voltage (V_{oc}) from these measurements wasn't possible.

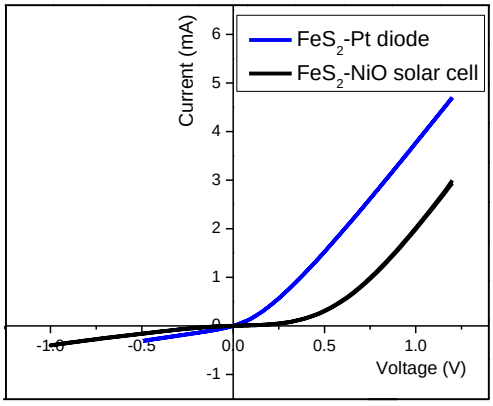

Figure 5. *I -V* curves of pyrite Schottky diode with Pt as junction partner (blue) and FeS_2/NiO heterojunction solar cell (black)

I-V curve of pyrite-FeS_2/NiO heterostructure is seen in Figure 5 (black). It is obvious that a junction between pyrite and SILAR deposited (20 cycles) NiO has been formed but no photocurrent is generated in this solar cell structure. The existence of pinholes or defects on pyrite crystals' surfaces could be responsible for the leakage current in reverse bias. Future studies are needed to improve the working ability of pyrite MGL solar cell structure.
Charge carrier concentrations found from *C-V* measurements were $6.2x10^{16}$ for FeS_2/NiO heterostructures and $2.5x10^{17}cm^{-3}$ for FeS_2/Pt Schottky diodes. These results are in good accordance with the expected values based on literature data [31].

6. Conclusions

FeS_2 monograin powder was considered as an option for absorber material in MGL solar cells for energy production in a future lunar habitat. In this work, the conditions for synthesis-growth of FeS_2 microcrystalline (monograin) powders and a cooling procedure for retaining the pyrite phase of FeS_2 without formation of additional phases were found. Synthesis of FeS_2 from FeS and S was performed at 600 ºC in the preheating step of synthesis-growth process followed by the recrystallization of FeS_2 crystals at 740 °C in molten KI

for a week. Slow cooling to 575 ºC and keeping the ampoule at this temperature for 24 hours followed by rapid cooling to room temperature resulted in single phase pyrite monograin powder. Produced FeS_2 had cubic structure with lattice parameters a = b = c = 5.4154 Å characteristic to the pyrite phase of FeS_2. Raman analysis (supported by XRD data) confirmed the pure pyrite phase. Powder crystals had round shape and *n-type* conductivity. Nearly half of the gained powder material was in the crystal size fraction of around 50 µm. Schottky diodes with Pt as junction partner showed a rectifying junction. First solar cells based on pyrite monograin powder in monograin layer design were assembled with *p*-type NiO. The pyrite/NiO device showed a formation of rectifying junction between the materials, but no photocurrent was detected. These results may be improved by further work with surface treatments of absorber material crystals and doping of pyrite.

Acknowledgements

This work has been supported by the European Regional Development Fund, Project TK141 and Mobilitas Pluss Returning Researcher Grant MOBTP131.

References

[1] M. Braun, N. G. Veronica Trivino, S. Hosseini, R. Schonenborg, and M. Landgraf, "Human lunar return: An analysis of human lunar exploration scenarios within the upcoming decade," *Acta Astronautica*, 2020, doi: 10.1016/j.actaastro.2020.03.037.

[2] J. N. Rasera, J. J. Cilliers, J. A. Lamamy, and K. Hadler, "The beneficiation of lunar regolith for space resource utilisation: A review," *Planetary and Space Science*. 2020. doi: 10.1016/j.pss.2020.104879.

[3] M. Braun, N. G. Veronica Trivino, S. Hosseini, R. Schonenborg, and M. Landgraf, "Human lunar return: An analysis of human lunar exploration scenarios within the upcoming decade," *Acta Astronautica*, 2020, doi: 10.1016/j.actaastro.2020.03.037.

[4] N. J. Bennett, D. Ellender, and A. G. Dempster, "Commercial viability of lunar In-Situ Resource Utilization (ISRU)," *Planetary and Space Science*, 2020, doi: 10.1016/j.pss.2020.104842.

[5] M. Altosaar *et al.*, "Monograin layer solar cells," 2003. doi: 10.1016/S0040-6090(03)00167-6.

[6] E. Mellikov *et al.*, "Monograin materials for solar cells," *Solar Energy Materials and Solar Cells*, 2009, doi: 10.1016/j.solmat.2008.04.018.

[7] E. Mellikov *et al.*, "Growth of CZTS-Based Monograins and Their Application to Membrane Solar Cells," in *Copper Zinc Tin Sulfide-Based Thin-Film Solar Cells*, 2015. doi: 10.1002/9781118437865.ch13.

[8] C. Leiner, C. Sommer, V. Satzinger, L. Plessing, and G. Peharz, "CPV membranes made by roll-to-roll printing: A feasible approach?," 2016. doi: 10.1063/1.4962100.

[9] T. Raadik, "Adapting Crystalsol product to a moon environment," *ESA GSTP Small Studies*, 2016. https://www.esa.int/Enabling_Support/Space_Engineering_Technology/Shaping_the_Future/Adapting_Crystalsol_product_to_a_moon_environment

[10] D. E. Wilhelms, "Lunar stratigraphy and sedimentology," *Icarus*, 1977, doi: 10.1016/0019-1035(77)90020-3.

[11] G. A. Landis, "Materials refining on the Moon," *Acta Astronautica*, 2007, doi: 10.1016/j.actaastro.2006.11.004.

[12] J. M. D. Day, E. M. M. E. van Kooten, B. A. Hofmann, and F. Moynier, "Mare basalt meteorites, magnesian-suite rocks and KREEP reveal loss of zinc during and after lunar formation," *Earth and Planetary Science Letters*, 2020, doi: 10.1016/j.epsl.2019.115998.

[13] M. Rahman, G. Boschloo, A. Hagfeldt, and T. Edvinsson, "On the Mechanistic Understanding of Photovoltage Loss in Iron Pyrite Solar Cells," *Advanced Materials*, 2020, doi: 10.1002/adma.201905653.

[14] C. Steinhagen, T. B. Harvey, C. J. Stolle, J. Harris, and B. A. Korgel, "Pyrite nanocrystal solar cells: Promising, or fool's gold?," *Journal of Physical Chemistry Letters*, 2012, doi: 10.1021/jz301023c.

[15] M. Limpinsel, "Limpinsel, M. (2015). Iron Pyrite Absorbers for Solar Photovoltaic Energy Conversion.," Irvine, 2015.

[16] M. Rahman, G. Boschloo, A. Hagfeldt, and T. Edvinsson, "On the Mechanistic Understanding of Photovoltage Loss in Iron Pyrite Solar Cells," *Advanced Materials*, 2020, doi: 10.1002/adma.201905653.

[17] R. V. Morris, "Origins and size distribution of metallic iron particles in the lunar regolith.," *Geochimica et Cosmochimica Acta, Supplement*, 1980.

[18] D. Vaniman, D. Pettit, and G. Heiken, "Uses of lunar sulfur," 1992.

[19] M. Altosaar *et al.*, "Monograin layer solar cells," 2003. doi: 10.1016/S0040-6090(03)00167-6.

[20] D. Shishin, E. Jak, and S. A. Decterov, "Critical Assessment and Thermodynamic Modeling of the Fe-O-S System," *Journal of Phase Equilibria*

and Diffusion, 2015, doi: 10.1007/s11669-015-0376-4.

[21] O. K. von Goldbeck, *IRON—Binary Phase Diagrams*. 1982. doi: 10.1007/978-3-662-08024-5.

[22] Y. Akaltun and T. Çayır, "Fabrication and characterization of NiO thin films prepared by SILAR method," *Journal of Alloys and Compounds*, vol. 625, Mar. 2015, doi: 10.1016/j.jallcom.2014.10.194.

[23] P. P. Altermatt, T. Kiesewetter, K. Ellmer, and H. Tributsch, "Specifying targets of future research in photovoltaic devices containing pyrite (FeS2) by numerical modelling," *Solar Energy Materials and Solar Cells*, 2002, doi: 10.1016/S0927-0248(01)00053-8.

[24] G. N. Derry and Z. Ji-Zhong, "Work function of Pt(111)," *Physical Review B*, 1989, doi: 10.1103/PhysRevB.39.1940.

[25] H. Vogt, T. Chattopadhyay, and H. J. Stolz, "Complete first-order Raman spectra of the pyrite structure compounds FeS2, MnS2 AND SiP2," *Journal of Physics and Chemistry of Solids*, 1983, doi: 10.1016/0022-3697(83)90124-5.

[26] A. N. Utyuzh, "Influence of temperature on raman spectra of the FeS2 single crystal with pyrite structure," *Physics of the Solid State*, 2014, doi: 10.1134/S1063783414100321.

[27] D. Shishin, E. Jak, and S. A. Decterov, "Critical Assessment and Thermodynamic Modeling of the Fe-O-S System," *Journal of Phase Equilibria and Diffusion*, 2015, doi: 10.1007/s11669-015-0376-4.

[28] A. Zavrazhnov, A. Naumov, A. Kosyakov, S. Berezin, V. Volkov, and A. Sergeeva, "The Iron Sulfides Crystal Growth from the Halide Melts," *Materials Research*, 2018, doi: 10.1590/1980-5373-mr-2017-0648.

[29] P. Prabukanthan, S. Thamaraiselvi, and G. Harichandran, " Single Step Electrochemical Deposition of p-Type Undoped and Co 2+ Doped FeS 2 Thin Films and Performance in Heterojunction Solid Solar Cells ," *Journal of The Electrochemical Society*, 2017, doi: 10.1149/2.0991709jes.

[30] H. Ning, Z. Liu, Y. Xie, and H. Huang, " CoS 2 Coatings for Improving Thermal Stability and Electrochemical Performance of FeS 2 Cathodes for Thermal Batteries ," *Journal of The Electrochemical Society*, 2018, doi: 10.1149/2.0321809jes.

[31] Z. Shi and A. H. Jayatissa, "Preparation and characterization of cobalt-doped iron pyrite (FeS2) thin films," *Progress in Natural Science: Materials International*, vol. 30, no. 3, Jun. 2020, doi: 10.1016/j.pnsc.2020.03.002.